Molecular dynamics of liquid SiO_2 under high pressure

James R. Rustad and David A. Yuen
Minnesota Supercomputer Institute and Department of Geology and Geophysics, University of Minnesota, Minneapolis, Minnesota 55455

Frank J. Spera
Department of Geological Sciences and Institute for Crustal Studies, University of California, Santa Barbara, California 93106
(Received 27 December 1989)

We have investigated with molecular dynamics the transport properties and velocity autocorrelation functions (VAF) for liqud SiO_2 up to pressures of 20 GPa and at temperatures of 4000 K using 252–1371 particles. A systematic study of the sensitivity of the self-diffusion coefficient to the number of particles in the system showed that around 800 are required for convergence. At low pressures the VAF reveals that motions of silicon and oxygen atoms are decoupled over the 50–75-fs range, across the second negative peak in the VAF of oxygen. As the pressure increases, the decoupling is shifted into the 25–50-fs range, over the first positive peak in the VAF of oxygen. In the spectral domain, the major feature on increasing pressure is the enhanced contribution of frequencies in the 800–1000-cm^{-1} region. This is consistent with high-pressure infrared spectroscopic measurements on silica glass. Analysis of the distribution of coordination numbers revealed that both the fivefold- and sixfold-coordinated silicon become prevalent between 7 and 20 GPa. This accords well with recent findings from NMR studies of silicate glasses. We propose that the importance of fivefold-coordinated states in determining the self-diffusion coefficient needs to be reassessed.

I. INTRODUCTION

One of the major successes in molecular-dynamics (MD) studies of silicate melts is the substantiation of Waff's[1] prediction that the self-diffusion coefficients (SDC) of network-forming species in silicate liquids increase with pressure. This anomalous behavior was verified experimentally by Kushiro,[2] and subsequent MD work on silica and alkali silicates by Woodcock, Angell, and Cheeseman[3] and Angell, Cheeseman, and Tamaddon[4] suggested the SDC's of Si and O increase with pressure, reaching a maximum at 12–15 GPa. These and later MD studies[5] of the pressure dependence of the SDC's in silicate liquids used fewer than 400 particles. It is well known that SDC's of simple liquids, as calculated by MD, depend significantly on the number of particles used in the simulations,[6] but no systematic analysis of the number dependence of the SDC's in silicate liquids has been carried out. To address this issue, we use a recent set of interatomic potentials derived from *ab initio* Hartree-Fock (HF) calculations due to Tsuneyuki *et al.*[7] (TTAM hereafter) to perform MD simulations investigating correlations in the motion of atoms in liquid SiO_2 at 4000 K up to pressures of 20 GPa using from 252 to 1371 particles. We present results concerning the coupled pressure and number dependence of the SDC's of silicon and oxygen as calculated from mean-squared displacement curves. Changes in the velocity autocorrelation function (VAF) with increasing pressure are described. We then discuss the populations of anomalously coordinated silicon and oxygen as a function of pressure and system size.

II. METHODS AND DESCRIPTION

We investigated the dynamics of pure SiO_2 liquids subject to the potentials given by TTAM for 252, 498, 864, and 1371 particles at pressures of 0, 7, 12, and 20 GPa at a temperature of 4000 K. Higher temperature runs would allow a more direct comparison with previous MD studies, but were not performed because of an instability involving pairs of oxygen atoms riding over their energy maxima at temperatures in excess of 5000 K. This is discussed below in more detail. All computations were performed on a CRAY X-MP 4/16. For 864 particles, the time required for one iteration was 0.54 sec.

The Si-O and O-O interactions of the TTAM potential are plotted in Fig. 1. The empirical potential of Woodcock, Angell, and Cheeseman[3] and a Born-Mayer-Huggins fit to a Hartree-Fock surface performed by Kubicki and Lasaga[5] are also plotted for comparison. The form for the potential of TTAM is

$$U_{ij}=\frac{Q_iQ_j}{r}+f_0(b_i+b_j)\exp\left[\frac{a_i+a_j-r}{b_i+b_j}\right]-\frac{c_{ij}}{r^6}\ , \qquad (1)$$

where r is the radial distance and f_0 is 1 kcal mol^{-1}. The parameters Q, a, b, and c are listed in Table I. The short-range attractive r^{-6} term causes the maxima in the Si-Si and O-O potentials at short range in Fig. 1.

The force loop was constructed using the method of Brode and Ahlrich,[8] which keeps all computational vectors of a length equal to the number of particles in the simulation. We used the velocity version of the Verlet algorithm[9] to integrate the equations of motion. A time step of 1.5 fs yielded energy conservation to one part in

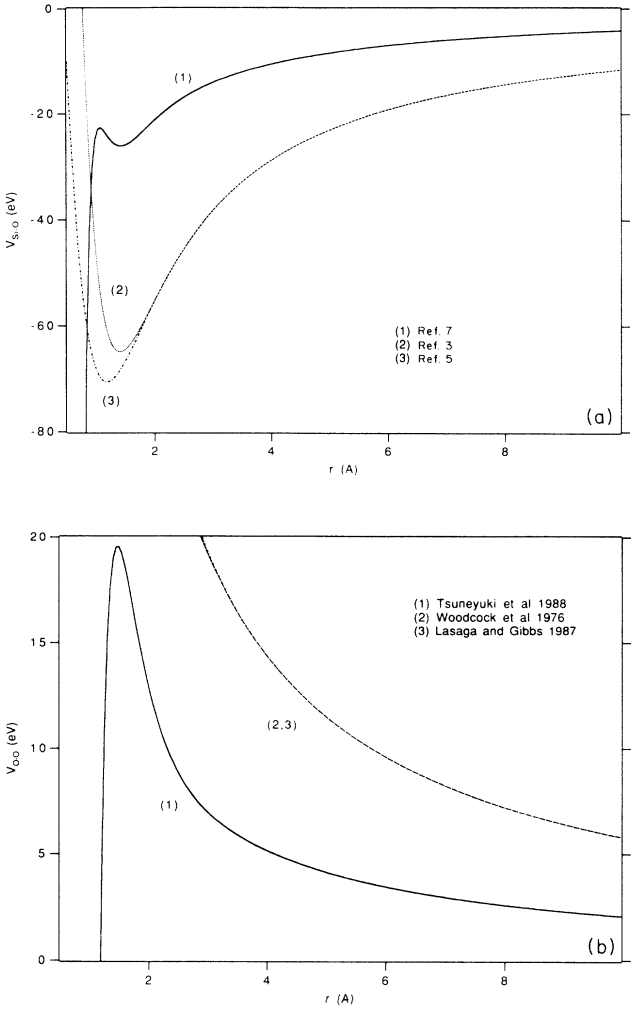

FIG. 1. Potential energy vs r for (a) Si-O interactions and (b) O-O interactions. Potentials of Tsuneyuki *et al.* (1) are used in this investigation. Those of Woodcock, Angell, and Cheeseman and Lasaga and Gibbs [(2) and (3), respectively] are presented for comparison.

10^5. The Coulomb energies and forces were summed using Ewald's method with $\alpha L = 5.74$, where α is the convergence factor for the Ewald sum and L is the length of the reference cell. The reciprocal space sum was terminated at $|\mathbf{h}|^2 < 52$, where $\mathbf{h}$ is a reciprocal lattice vector in units of $2\pi L^{-1}$.

The computations started from an fcc lattice and were then randomized at 15 000 K. They were cooled incrementally from 15 000° to 4500° at the rate of 1° per time step at zero pressure using the velocity and pressure scaling method of Berendsen *et al.*[10] Pressures were calculated in real space using the expression

$$PV = Nk_B T - \tfrac{1}{3} \sum_i \sum_{j\,(>i)} \mathbf{r}_{ij} \cdot \mathbf{f}_{ij} \,, \tag{2}$$

where N is the number of particles, $\mathbf{r}_{ij}$ is the distance between the i,jth pair, and $\mathbf{f}_{ij}$ is the force on i due to j. A wave-number space correction was added having the form

$$P_k V = -\tfrac{1}{3} \sum_i \mathbf{r}_i \cdot \mathbf{f}_{i_k} \,, \tag{3}$$

where P_k is the pressure from reciprocal space and $\mathbf{f}_{i_k}$ is the total force on atom i due to the wave-number space sum.

After each increment of 1000 deg of cooling, the system was allowed to equilibrate at constant energy and volume for 200 time steps. Because of the relatively low energy maxima due to the r^{-6} attractive term, we used the parameters of Soules[11] during the high-temperature phase of equilibration. At a temperature of 4500 K the TTAM parameters were substituted for the Soules parameters and the system was cooled to the run temperature of 4000 K over 500 time steps. The calculation was then allowed to stabilize for 5000 time steps at constant volume and energy appropriate to approximately zero pressure and 4000 K. The desired pressure was achieved using coordinate scaling, allowing equilibration to new pressures every 1 GPa of pressure increase until the density did not appear to be drifting systematically. Typically this took 300–500 time steps. After the density had stabilized, the system was held at constant temperature and volume for 250 time steps and at constant energy and volume for 1000 time steps.

The mean-squared displacement of the atoms as a function of time, the VAF, and a histogram of the coordination numbers of silicon and oxygen were obtained from the simulations. All data were collected in the NEV (constant number of particles, energy, and volume) MD ensemble. The mean-squared displacement functions were collected over 3000 fs and were averaged over 250 different time origins separated in time by 15 fs. The VAF's were collected over 600 fs and were averaged over 1000 time origins separated by 1.5 fs. The histograms of the coordination statistics represent averages over 750 fs.

TABLE I. Potential parameters of Eq. (1) from Tsuneyuki *et al.* (Ref. 7).

	Q/e	a (Å)	b (Å)	c (kcal$^{1/2}$ Å^3 mol$^{-1/2}$)
O	−1.200	2.0474	0.175 66	70.37
Si	+2.400	0.8688	0.032 85	23.18

III. RESULTS AND DISCUSSION

A. Mean-squared displacement curves

Graphs showing the mean-squared displacement with time as a function of the number of particles and pressure are displayed in Figs. 2 and 3. The SDC's were computed using a least-squares fit to the data in the 500–3000-fs range and are plotted in Fig. 4. These SDC's are quite high compared to those calculated in other MD studies using empirical potentials,[3,4,12] giving values at 4000 K similar to those given by others at 6000 K. Figures 2 and 3 show that at high pressure the mean-squared displacement versus time curves for the 252 atom case do not converge to a well-defined slope at long times. Therefore

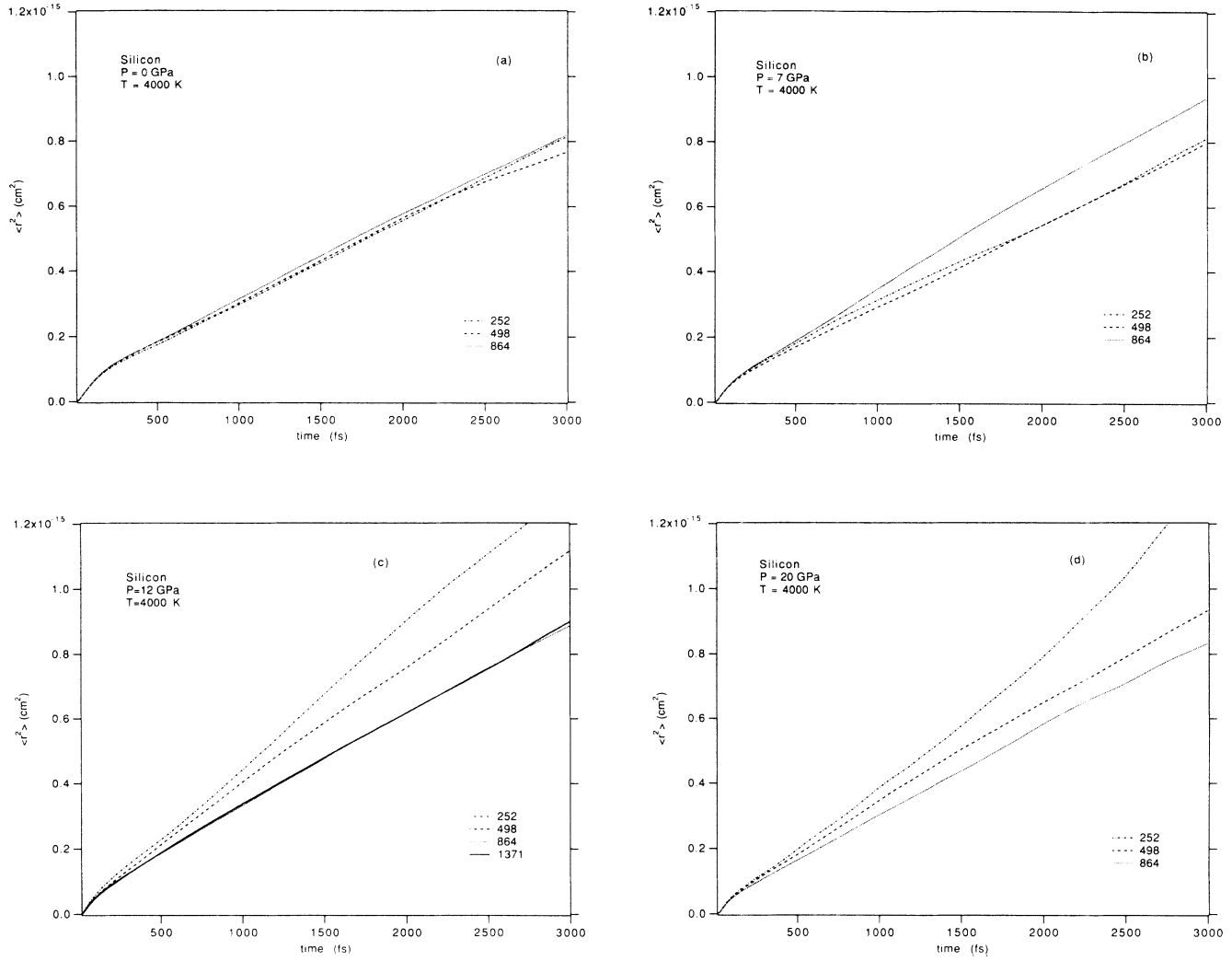

FIG. 2. Mean-squared displacement vs time of silicon atoms at 4000 K for system sizes of 252, 498, and 864 particles at pressures of (a) 0, (b) 7, and (d) 20 GPa. (c) is at 12 GPa and includes runs using 252, 498, 864, and 1371 particles. Time is in units of femtoseconds. Curves represent averages over 250 time origins separated by 15 fs.

these runs never reached an equilibrium state and a diffusion coefficient cannot be strictly defined. A tentative diffusion coefficient was assigned using the same procedures as in the other systems. These results, summarized in Fig. 4, strongly suggest that as the size of the system increases, the amplitude of the diffusivity maximum decreases, and there is some indication that the position of the maximum is shifted to lower pressures. For small systems, our results are in agreement with previous MD studies[3,4] of this pressure maximum (using up to 324 atoms) in terms of both its amplitude and its position. As we attempted to increase the size of the system beyond 864, an instability developed which would infrequently allow an oxygen atom to move over the potential maximum of another oxygen atom [see Fig. 1(b)]. These events were carefully recalculated using smaller time steps with and without the Ewald sum routine, in order to check the numerical methods. The event was not affected by these changes and energy conservation improved by the amount expected for smaller time steps,[9] which we took as good evidence for the correctness of our code. At 12 GPa we were able to complete a run for 1371 particles using the same averaging procedures as described for the systems of smaller size. The convergence of the results with increasing numbers of particles in Figs. 2(c) and 3(c) is convincing and suggests that 864 particles are sufficient to determine the diffusion behavior of SiO_2 systems under pressure. We find that at low pressures the properties of the system do not strongly depend on the number of particles used; this agrees with Mitra's work[12] carried out at low pressure using up to 3000 particles.

B. Velocity autocorrelation function

The velocity autocorrelation function is defined as

$$Z(t)=\frac{1}{N}\sum_i \frac{\mathbf{v}_i(t)\cdot\mathbf{v}_i(0)}{\mathbf{v}_i(0)\cdot\mathbf{v}_i(0)}\ , \tag{4}$$

where N is the number of particles and $\mathbf{v}_i$ is the velocity

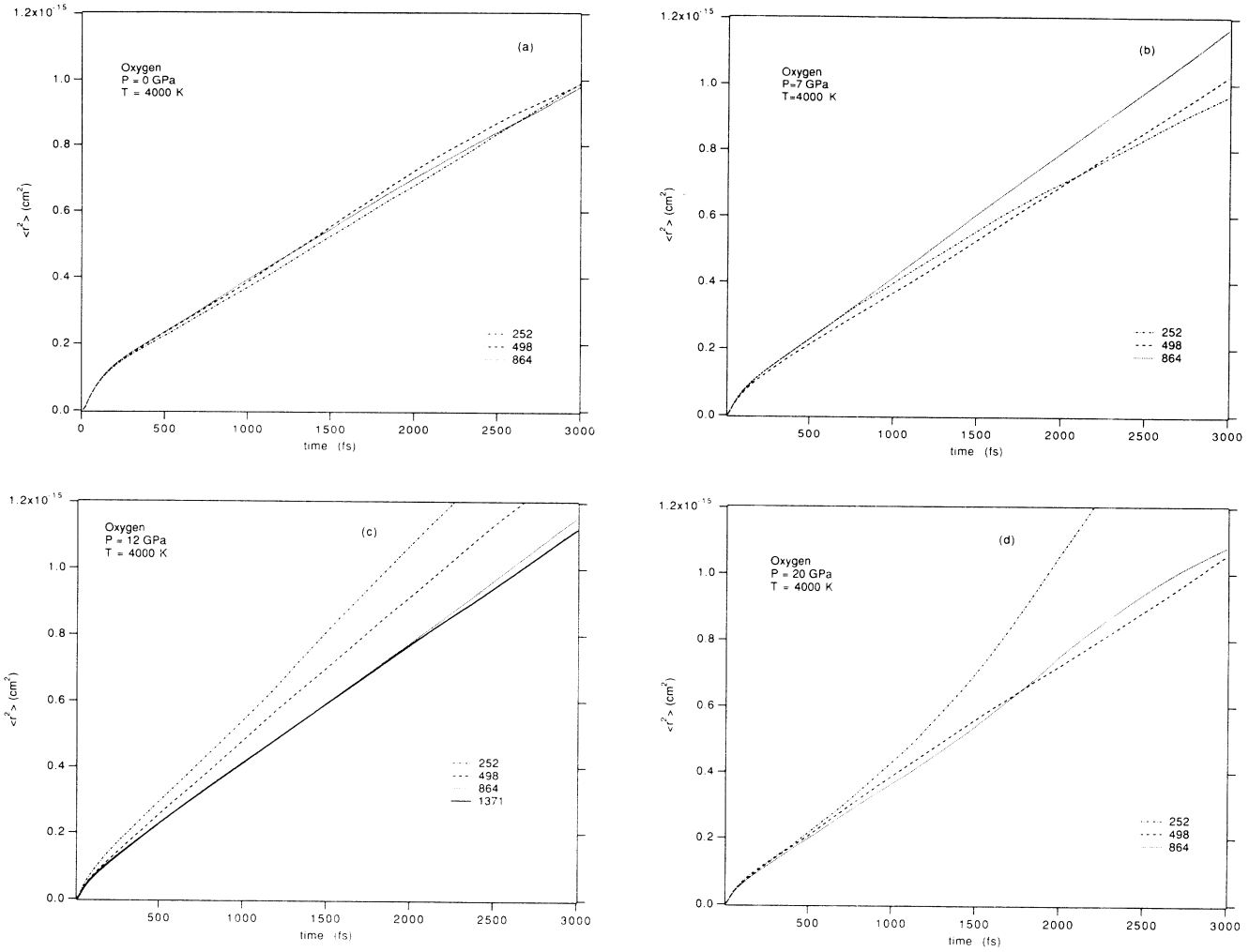

FIG. 3. Mean-squared displacement vs time of oxygen atoms at 400 K for system sizes of 252, 498, and 864 particles at pressures of (a) 0, (b) 7, and (d) 20 GPa. (c) is at 12 GPa and includes runs using 252, 498, 864, and 1371 particles. Time is in units of femtoseconds. Curves represent averages over 250 time origins separated by 15 fs.

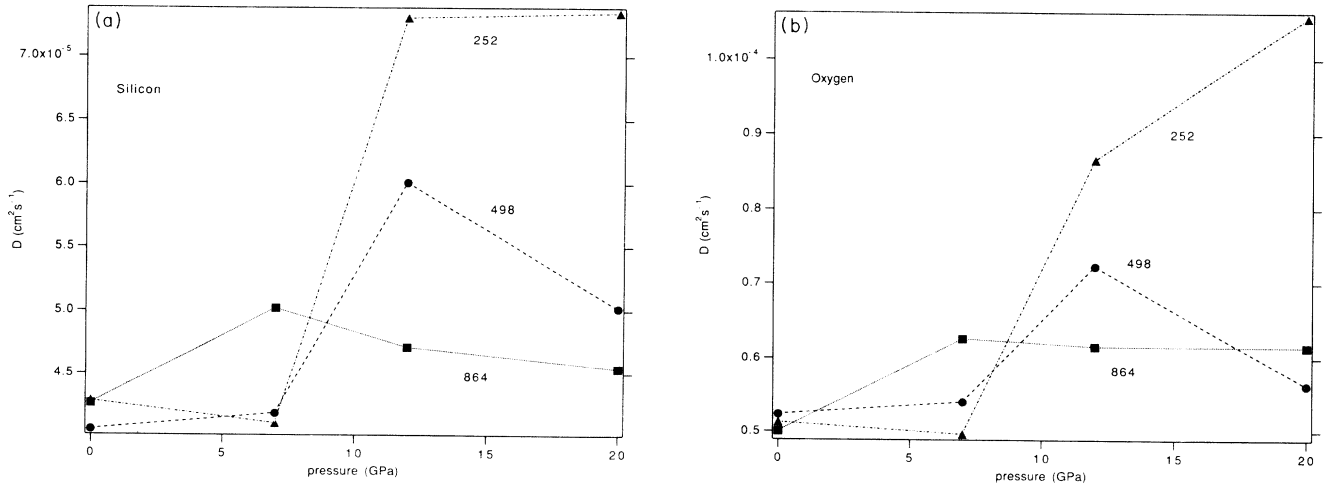

FIG. 4. Self-diffusion coefficients vs pressure for (a) silicon and (b) oxygen. Triangles represent simulations using 252 particles, circles represent those using 498 particles, and squares represent those using 864 particles. Time is in units of femtoseconds. These values represent least-squares fits to the mean-squared displacement curves over the 500–3000-fs range.

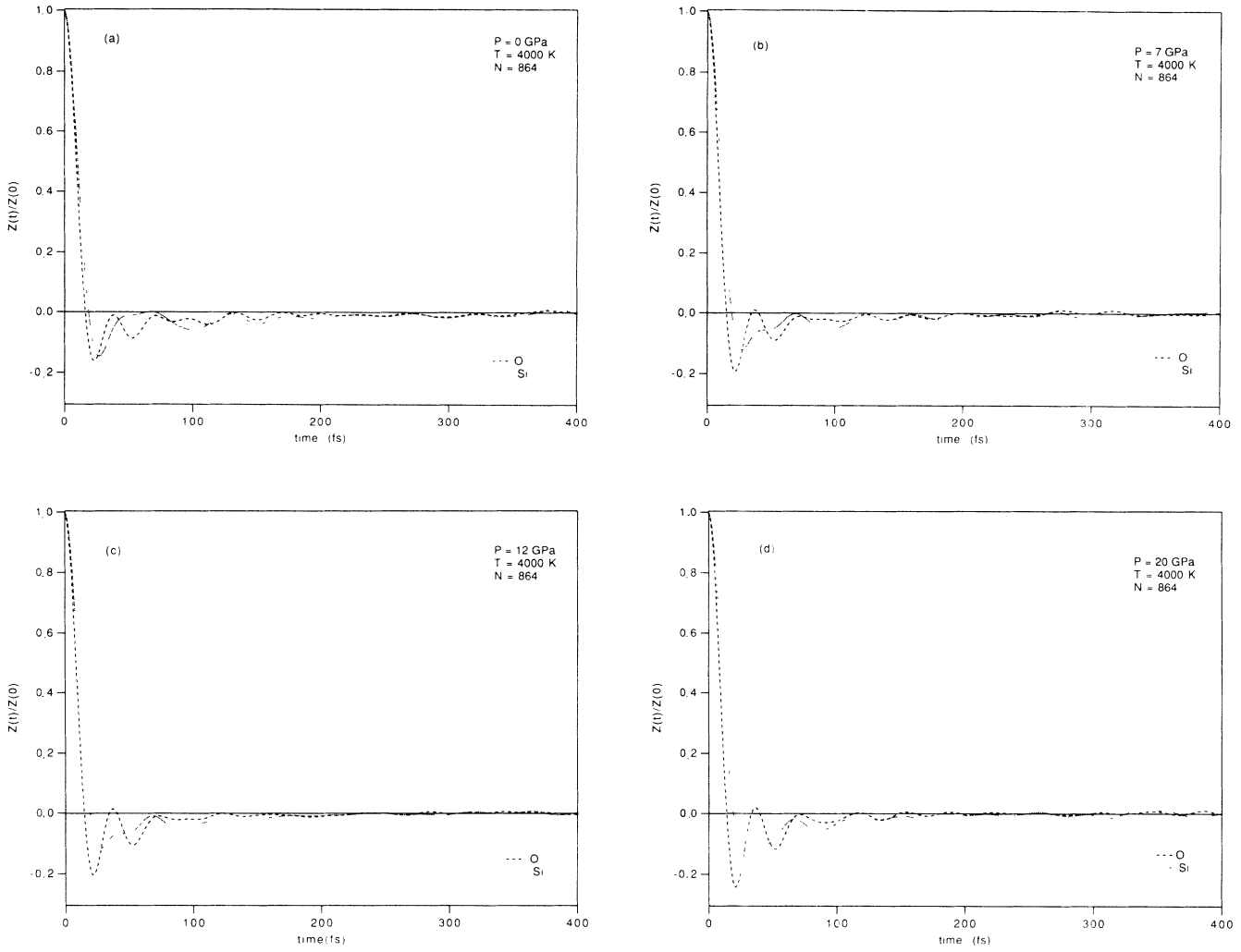

FIG. 5. Velocity autocorrelation function for a system of 864 particles at 4000 K under pressures of (a) 0 GPa, (b) 7 GPa, (c) 12 GPa, and (d) 20 GPa. Time is in units of femtoseconds. These curves are the result of averages taken over 1000 time origins separated by 1.5 fs.

of particle i. In principle, the velocity autocorrelation function can also be used to determine the SDC, but the long-time tail giving small, systematic contributions to the SDC is easily swamped by noise.[6] However, the VAF is useful for examining short-time behavior of atomic motions. In Fig. 5, the VAF is plotted for the 864-particle system for 0, 7, 12, and 20 GPa. As the pressure increases, the amplitude of the first negative peak for oxygen atoms is increased and shifted slightly to shorter time indicating a decrease in size and an increase in the effectiveness of the ionic cage which surrounds the oxygen atoms. For silicon the situation is reversed, with an increase in pressure decreasing slightly the backscattering amplitude and moving the minimum to slightly longer times. The first negative peak is also much broader in silicon at high pressure, extending over the 50–80-fs range. This is probably related to the presence of a larger cage of higher coordination number around the silicon atom. The VAF at 0 GPa exhibits a much longer negatively correlated region than those at higher pressures, going out to 375 fs, as opposed to 200 fs for the higher-pressure cases. In addition, the oxygen and silicon VAF's are out of phase at earlier times at high pressures. The out-of-phase region extends from 50 to 75 fs at 0 pressure, but gradually moves to shorter times, covering the 25–50-fs ranges at 20 GPa.

The power spectrum of the VAF, defined as

$$f(\omega)=\frac{6}{\pi}\int_0^\infty Z(t)\cos(\omega t)dt \ , \tag{5}$$

is displayed in Fig. 6 for oxygen and silicon at 0, 12, and 20 GPa. In taking the transforms, zeros were added to the 400-time-step (600 fs) time series to reach 512, the next power of 2, in accordance with the fast-Fourier-transform algorithm.[13] Although our runs were performed at significantly higher temperatures, the shape of the spectral representation of the VAF is similar to that

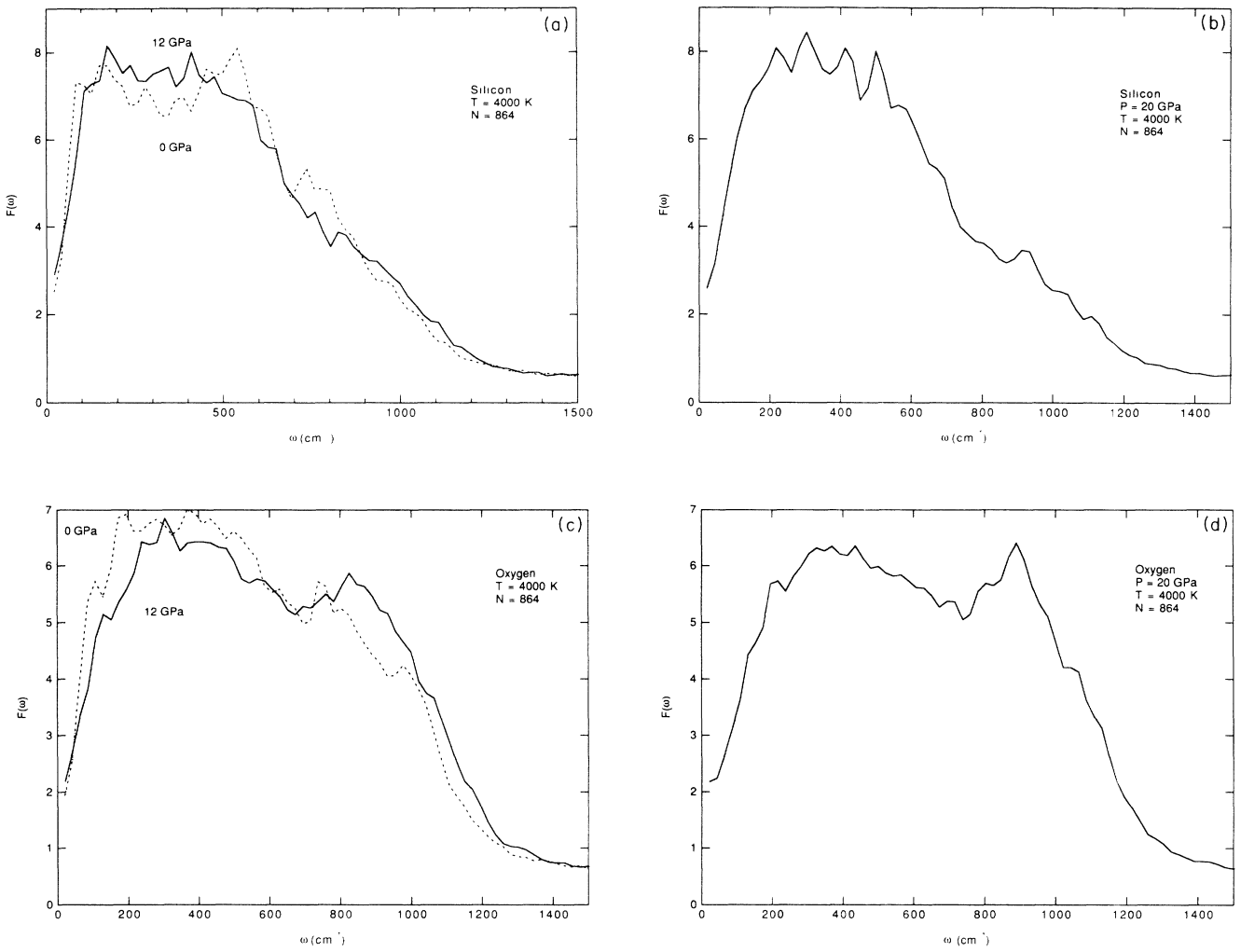

FIG. 6. Frequency spectrum $F(\omega)$ of the velocity autocorrelation function at 4000 K using 864 particles for (a) silicon atoms at 0 and 12 GPa, (b) silicon atoms at 20 GPa, (c) oxygen atoms at 0 and 12 GPa, and (d) oxygen atoms at 20 GPa.

found experimentally by Williams and Jeanloz[14] in a study of the infrared absorption characteristics of silica glass at high pressures and room temperature. They found that increasing pressures result in increasing intensity of infrared absorption in the region between 600 and 900 cm^{-1} and a drop in the intensity at the peak near 1100 cm^{-1}. The potentials used here predict larger contributions to the VAF frequency spectrum in the region between 800 and 900 cm^{-1} in accordance with these experiments. The reason for the lack of a strong peak at 1100 cm^{-1} is not clear. It is unlikely that the discrepancy is due to temperature, but may possibly indicate that these potentials are better suited to octahedral coordinations. For silicon, the main changes in the transformed VAF with increasing pressure are (i) the two broad peaks near 200 and 600 cm^{-1} at 0 GPa merge into a broad single peak near 400 cm^{-1} at 20 GPa and (ii) the peak centered near 800 cm^{-1} at 0 GPa consistently increases in frequency as pressure increases but has a smaller amplitude in the 12 GPa run than in the 0 or 20 GPa runs. This behavior is manifested as a smoother approach to zero correlation in the time domain and is near the Si-O stretching frequency.[12] For oxygen the main feature is a monotonic decrease in the intensity of the broad peak centered near 400 cm^{-1} with pressure and a concomitant increase in the intensity of the peak near 900 cm^{-1}. Both peaks are shifted towards higher frequencies. There is a small shoulder on the large oxygen peak at 1000 cm^{-1} that behaves similarly to the peak at 800 cm^{-1} in the silicon spectrum.

C. Structure and changes in coordination number

The effect of pressure on the radial distribution function $g(r)$ is shown in Fig. 7 where $g(r)$ is plotted for 0 and 20 GPa. The radial distribution function is somewhat insensitive to pressure. The major changes are an increase in the number of Si—O bonds in the region of the first minimum in $g(r)$, a broader distribution of Si-Si distances, and a shift of O-O distances to smaller values.

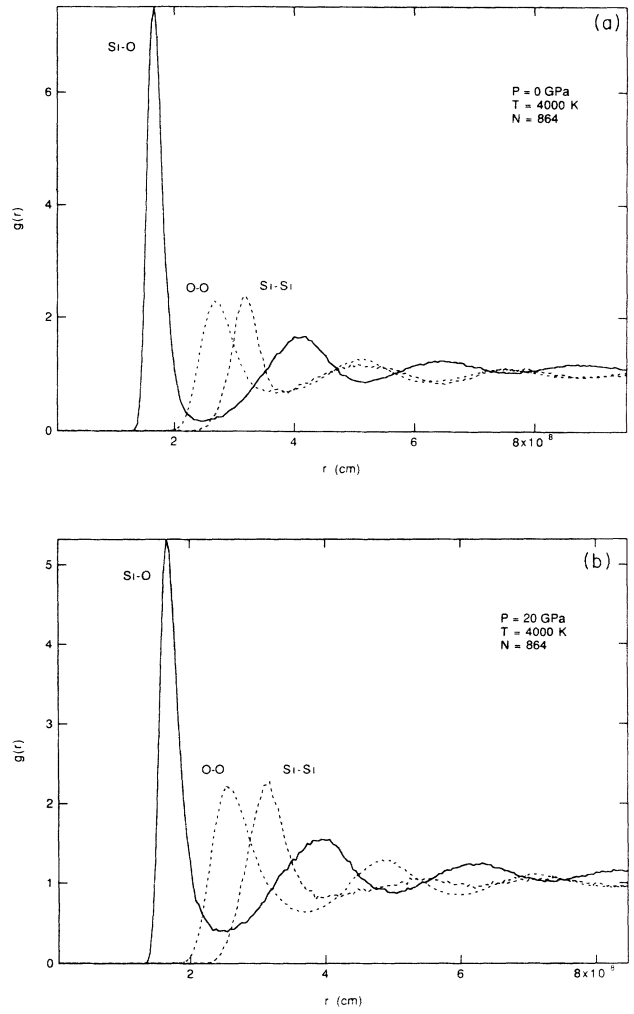

FIG. 7. Radial distribution functions for Si-O, O-O, and Si-Si pairs for the 864-particles system at 4000 K at pressures of (a) 0 GPa and (b) 20 GPa.

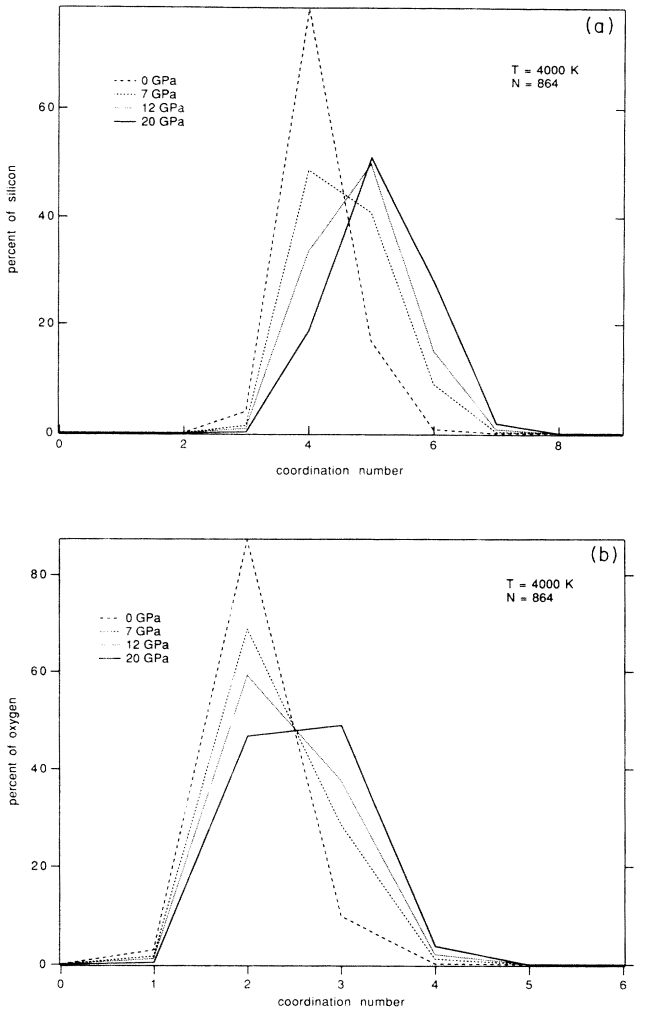

FIG. 8. Coordination statistics at pressures of 0, 7, 12, and 20 GPa for the 864-particle system at 4000 K. Table II shows a comparison of these numbers to coordination numbers taken from the 252-particle system.

Several MD studies have demonstrated a positive correlation between the diffusivity maximum for silicon and oxygen and the populations of fivefold-coordinated silicon and threefold-coordinated oxygen.[3–5,15] This study suggests that the magnitude of the diffusivity maximum is dependent on the size of the system investigated. We find that system size did not significantly affect the distribution of coordination numbers, as shown in Table II. The effect of pressure on the coordination distribution is strong. The changes in oxygen and silicon coordination with pressure for the 864 particle case are summarized in Fig. 8. The first minimum in $g(r)$ was used as the cutoff for the first coordination sphere. This figure reveals large amounts of fivefold-coordinated silicon even at low pressures using this criterion. The percentage of fivefold-coordinated Si increases by 25% as the pressure increases from 0 to 7 GPa, but only increases 10% from 7 to 20 GPa. Beyond 7 GPa most of the loss of fourfold-coordinate silicon is accounted for by an increase in octahedral silicon with the amount of fivefold-coordinated Si remaining relatively constant. Although the percentages of fivefold-coordinated Si are higher in our study, most of the increase in fivefold-coordinated Si occurs within 10 GPa, which is consistent with recent NMR studies of alkali-metal silicate glasses quenched from high pressures.[16,17] Changes in oxygen coordination are more regular; twofold-coordinated oxygen becomes threefold coordinated in a continuous manner with increasing pressure. Though we do find a maximum in the concentration of fivefold-coordinated Si at 12 GPa for all system sizes, this maximum is not associated with a significant increase in the diffusion coefficient at 12 GPa for the 864-particle case. Color snapshots of the 498-particle system are displayed in Fig. 9 (oxygen atoms are magenta and silicons are gray). Although the periodic boundaries and perspective can give the appearance of cutting the edges and corners off unevenly, it is clear the tetrahedral structure is better developed in the low-pressure case, whereas in the high-pressure cases the coordination geometry is more irregular and there is a visible tendency

TABLE II. Coordination statistics for the 864- and 252-particle systems (N is the coordination number). Data were collected over 750 fs. Results for the 252-particle system are in parentheses.

N	0 GPa (%)	7 GPa (%)	12 GPa (%)	20 GPa (%)
		Silicon		
0	0 (0)	0 (0)	0 (0)	0 (0)
1	0 (0)	0 (0)	0 (0)	0 (0)
2	0 (0)	0 (0)	0 (0)	0 (0)
3	4 (6)	1 (1)	1 (1)	0 (0)
4	78 (77)	49 (45)	34 (36)	19 (22)
5	17 (16)	41 (42)	49 (48)	51 (49)
6	1 (1)	9 (12)	15 (15)	48 (27)
7	0 (0)	0 (0)	1 (0)	2 (2)
8	0 (0)	0 (0)	0 (0)	0 (0)
		Oxygen		
0	0 (0)	0 (0)	0 (0)	0 (0)
1	3 (3)	2 (1)	1 (1)	0 (1)
2	87 (88)	69 (67)	59 (67)	47 (47)
3	10 (9)	28 (31)	38 (36)	49 (49)
4	0 (0)	1 (1)	2 (2)	4 (3)
5	0 (0)	0 (0)	0 (0)	0 (0)

towards higher coordination with some octahedra visible. Note the nonhomogeneous distribution of free volume in the low-pressure case.

We have also employed visualization techniques to study the dynamics of coordination changes in live action. By viewing these processes in animation we have gained insight into the coordination changes within the context of collective vibratory movements of the ensemble of atoms. One can discern the differences in structure as a function of pressure. At high pressures octahedral structures can be observed vividly. Copies of the video are available upon request to the authors.

IV. SUMMARY AND DISCUSSION

In this work we have described the changes which occur in liquid silica at a temperature of 4000 K as the pressure is increased from 0 to 20 GPa. Our data suggest that the nature of the pressure-induced maximum in the self-diffusion coefficients for both oxygen and silicon are dependent on the system size, the amplitude of the maximum being decreased and shifted to lower pressures for larger systems. Differences in the behavior of the velocity autocorrelation function with increasing pressure were described in both the time and frequency domains. It was demonstrated that at higher pressures the duration of the first backscattering peak in the velocity autocorrelation function for silicon was extended but the time necessary to relax to near zero from the negatively correlated region was decreased. Higher pressures increase the population of fivefold- and sixfold-coordinated silicon, in a manner which is consistent with previous MD studies and NMR experiments. The drop in the amplitude of the diffusivity maximum for the large systems

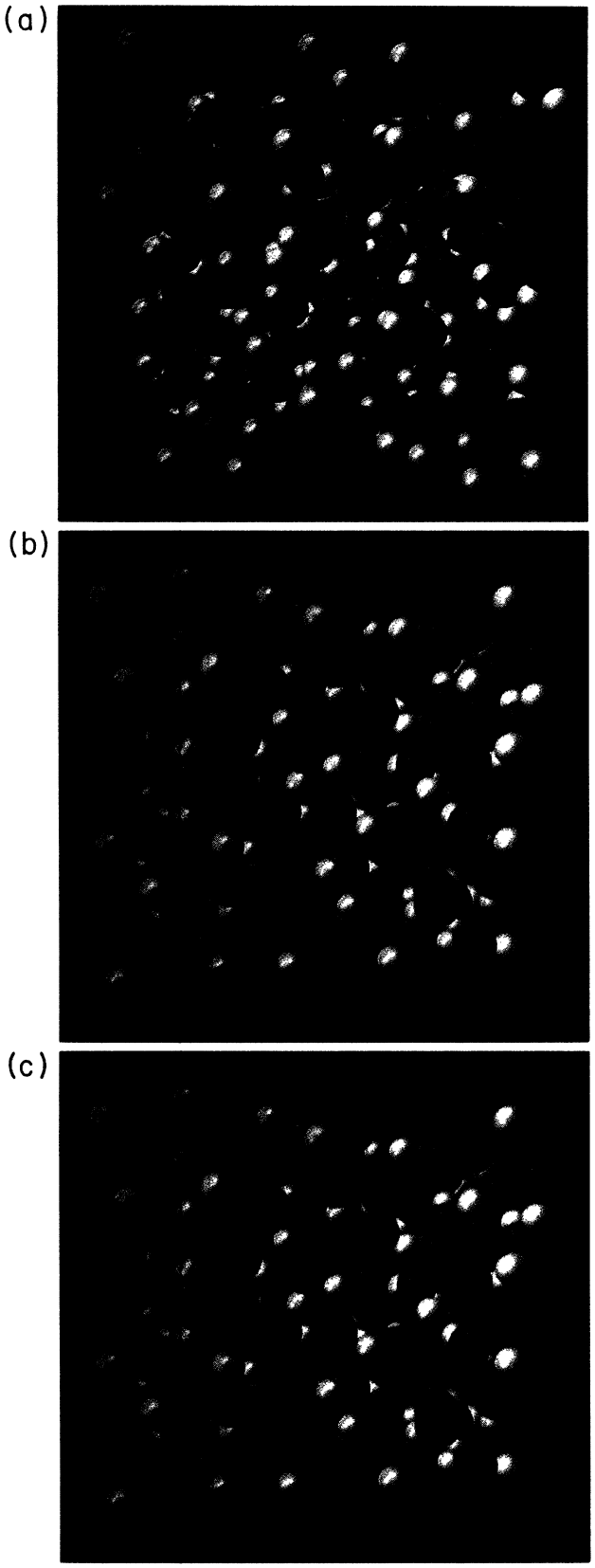

FIG. 9. Snapshots of the liquid structure of the 498-particle system at 4000 K under pressures of (a) 0 GPa (density=2.3 g cm^{-1}), (b) 12 GPa (density=3.12 g cm^{-3}), and (c) 20 GPa (density=3.49 g cm^{-3}). Silicon atoms are grey and oxygen atoms are magenta.

could not be correlated with any major change in the coordination statistics, indicating that factors other than coordination number may be important in determining the nature of diffusive atomic motions.

Future work is planned to address the question of whether the results obtained here depend on the specific potentials used. If the results concerning system-size dependence are valid in general, then some larger-scale mechanisms, which do not necessarily depend on fivefold-coordinated Si, are operative in determining the diffusion process. The high diffusion coefficients predicted by these potentials may result from the inaccuracies of fitting potential parameters to HF surfaces calculated for near equilibrium cluster configurations. Liquid systems move over a large region of the potential surface and involve the breaking and forming of chemical bonds. More data are needed at larger atomic separations to better constrain the potential surface far from equilibrium. The potentials used here do indicate anomalous behavior in the 12-GPa range even for large systems, as revealed in the coordination data and by the faster decay of the velocity autocorrelation functions. The VAF behavior consistent with a higher diffusion coefficient for the 12-GPa system, but the long-time behavior of the larger systems appears to conspire against a larger diffusion coefficient. If it is found that this phenomenon is peculiar to the potential used here, it would then be useful to know what aspects of the potential produce such behavior, as the pressure-induced structural changes and thermodynamic properties are predicted well by these potentials.[7,18]

ACKNOWLEDGMENTS

This research was supported by NASA (Graduate Student Researchers Program) (J.R.R.) and National Science Foundation Grants No. EAR 86-08479 and No. EAR 88-17200.

[1]H. S. Waff, Geophys. Res. Lett. **2**, 193 (1975).
[2]I. Kushiro, J. Geophys. Res. **81**, 6347 (1976).
[3]L. V. Woodcock, C. A. Angell, and P. A. Cheeseman, J. Chem. Phys. **65**, 1565 (1976).
[4]C. A. Angell, P. A. Cheeseman, and S. Tamaddon, Science **218**, 885 (1982).
[5]J. D. Kubicki and A. C. Lasaga, Am. Mineral **73**, 941 (1988).
[6]B. J. Alder and T. E. Wainwright, Phys. Rev. A **1**, 18 (1970).
[7]S. Tsuneyuki, M. Tsukada, H. Aoki, and Y. Matsui, Phys. Rev. Lett. **61**, 869 (1988).
[8]S. Brode and R. Ahlrichs, Comput. Phys. Commun. **42**, 51 (1986).
[9]M. P. Allen and D. J. Tildesley, *Computer Simulation of Liquids* (Clarendon, Oxford, 1987).
[10]H. J. C. Berendsen, J. P. M. Postma, W. F. Van Gunsteren, A. Nicola, and J. R. Haak, J. Chem. Phys. **81**, 3684 (1984).
[11]T. F. Soules, J. Non-Cryst. Solids **49**, 39 (1982).
[12]S. K. Mitra, Philos. Mag. B **45**, 529 (1982).
[13]W. H. Press, B. P. Flannery, S. A. Teukolsky, and W. T. Vetterling, *Numerical Recipes* (Cambridge University Press, New York, 1986).
[14]Q. Williams and R. Jeanloz, Science **239**, 902 (1988).
[15]S. Brawer, *Relaxation in Viscous Liquids and Glasses* (American Ceramic Society, Columbus, 1985).
[16]X. Xue, J. F. Stebbins, M. Kanzaki, and R. G. Tronnes, Science **245**, 965 (1989).
[17]J. F. Stebbins and P. McMillan, Am. Mineral **74**, 765 (1989).
[18]S. Tsuneyuki, Y. Matsui, H. Aoki, and M. Tsukada, Nature **339**, 209 (1989).

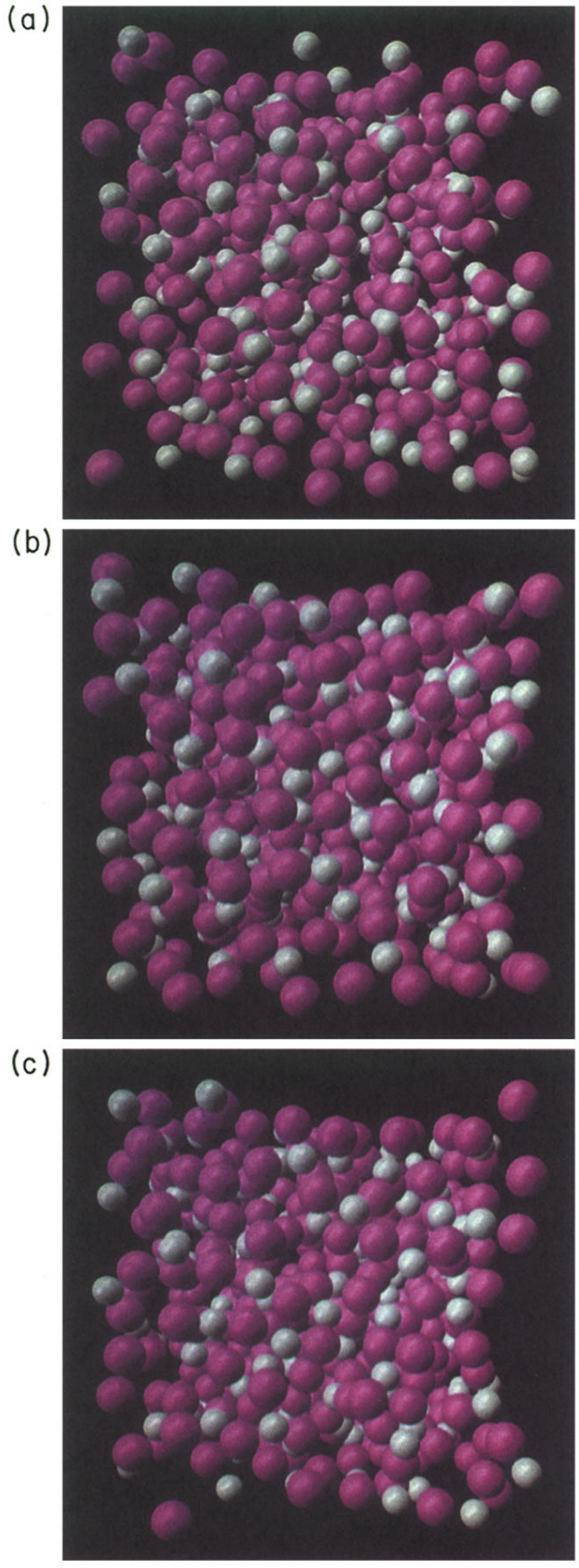

FIG. 9. Snapshots of the liquid structure of the 498-particle system at 4000 K under pressures of (a) 0 GPa (density = 2.3 $g\,cm^{-1}$), (b) 12 GPa (density = 3.12 $g\,cm^{-3}$), and (c) 20 GPa (density = 3.49 $g\,cm^{-3}$). Silicon atoms are grey and oxygen atoms are magenta.